

# Structural and thermoelectric power studies of citrate-gel-prepared cobalt-substituted lithium nanoferrites

G. Aravind · M. Raghasudha · D. Ravinder ·  
Abdul Gaffoor · V. Nathanial

Received: 13 September 2014 / Accepted: 10 November 2014 / Published online: 10 December 2014  
© The Author(s) 2014. This article is published with open access at Springerlink.com

**Abstract** Nanocrystalline lithium cobalt ferrites of compositions  $[\text{Li}_{0.5}\text{Fe}_{0.5}]_{1-x}\text{Co}_x\text{Fe}_2\text{O}_4$  (where  $x = 0.0, 0.2, 0.4, 0.6, 0.8$ , and  $1.0$ ) were synthesized at lower processing temperature ( $180^\circ\text{C}$ ) by non-conventional citrate gel autoignition method using citric acid as a fuel and oxidant. Structural characterization of the sintered samples was carried out by X-ray diffraction (XRD) analysis, FTIR spectroscopy, and transmission electron microscopy (TEM). XRD studies of the prepared samples confirmed the homogeneous single-phase cubic spinel structure with the crystallite sizes ranging from 37 to 43 nm. FTIR studies also revealed the formation of ferrites showing two significant absorption bands. The high-frequency band ( $\nu_1$ ) around  $600\text{ cm}^{-1}$  was attributed to the intrinsic vibration of tetrahedral complexes, and the low-frequency band ( $\nu_2$ ) around  $400\text{ cm}^{-1}$  was due to the octahedral complexes. TEM images showed the agglomeration of the particles with an average particle size of 30 nm. Thermoelectric power (TEP) studies of the prepared samples were carried out from 200 to  $600^\circ\text{C}$  using a differential method. The variation of Seebeck coefficient ( $S$ ) with temperature indicated p-type semiconducting nature of the sample at lower temperature and n-type semiconducting nature at

higher temperature indicating the conduction due to the electrons. The Curie temperature ( $T_c$ ) of the prepared samples measured from TEP studies showed a decreasing trend with the increasing Cobalt concentration.

**Keywords** Citrate gel autocombustion method · Nanoferrites · TEM image · Seebeck coefficient · Thermoelectric power

## Background

Nanosized ferrimagnetic oxides technically called ferrites have attracted considerable attention, not only out of a fundamental scientific interest but also from the practical point of view. This may be due to their growing applications in the electronic and microwave field. The special feature of these materials is that their properties can be tailored by appropriate substitution of different transition/rare earth ions in the chemical formula unit and through control of processing procedures.

Transition metal oxide nanoparticles, i.e., nanoferrites have been extensively investigated due to their unique catalytic, electric, and magnetic properties compared to those of their bulk counterparts, and the wide range of their potential applications [1]. Among these materials, spinel ferrites were industrially important materials with commercial value. They find extensive applications in the form of various passive components in electric, electronic, and microwave devices [2]. The basis for the wide range of applications is related to the variety of transition metal cations which can be incorporated into the lattice of the parent magnetic structure [3]. The introduction of transition metal ions modifies the properties of the ferrites in accordance with the desired purpose.

G. Aravind · D. Ravinder · A. Gaffoor  
Department of Physics, Osmania University,  
Hyderabad 500007, Telangana, India

M. Raghasudha (✉)  
Department of Chemistry, Jayaprakash Narayan College of  
Engineering, Mahabubnagar 509001, Telangana, India  
e-mail: raghasudha\_m@yahoo.co.in

V. Nathanial  
Department of Physics, University College of Science,  
Osmania University, Sifabad, Hyderabad, Telangana, India



In the olden days, microwave devices were based on the garnets, but due to the low Curie temperature ( $T_c$ ) and high cost, these garnets are replaced by the lithium ferrites. In lithium ferrites, lithium ions and some of the iron ions occupy the octahedral site, while the remaining iron ions occupy the tetrahedral site [4, 5]. In order to have a high degree of molecular mixing, chemical homogeneity, stoichiometric control, and low sintering temperature/time, various chemical methods have been used for the preparation spinel ferrites [6–8]. Out of the various existing synthesis methods, citrate-gel autocombustion method has attracted great interest because of its inherent advantages in achieving the aforesaid properties. Until now, various investigations have been carried out to make further developments in the structural and electric properties of substituted lithium ferrites. The transition metal ions are becoming promising substituents for the improvement of the ferrite properties. Many researchers have studied the influence of various transition metal ions doping on the properties of lithium ferrites like Li–Ni [9], Li–Zn [10], and Li–Cd [11].

Hall coefficient measurement and thermoelectric power studies were widely used in the interpretation of conduction mechanism in ferrites. However, in the case of ferrites, it is somewhat difficult to measure Hall effect with high precision. In such cases, thermoelectric power measurement was one of the alternatives [12]. To the authors' knowledge, there is scarce information in the literature on the electric transport properties of cobalt-substituted lithium ferrites.

The objective of the present work is to prepare the nanocrystalline cobalt-substituted lithium ferrites at low sintering temperature through Citrate-gel autocombustion method. The crystallographic structure/microstructure was investigated by means of X-ray diffraction (XRD), fourier transform infra red spectroscopy (FTIR), and transmission electron microscopy (TEM). Thermoelectric power (TEP) studies of the prepared samples were carried out by means of a differential method in the temperature range of 200–600 °C.

## Results and discussion

The average crystallite size of the prepared samples were calculated from the measured width of their diffraction curve using Debye–Scherrer's formula [13]

$$D = \frac{0.91\lambda}{\beta \cos \theta} \quad (1)$$

where  $\lambda$  is the wavelength of the X-ray used, and  $\beta$  is the full-width half-maximum (FWHM) in radians. The lattice

constant  $a$  can be calculated using the following formula [13]:

$$a = d\sqrt{h^2 + k^2 + l^2} \quad (2)$$

where  $d$  is the interplanar distance which can be obtained from the Bragg's equation.

Hopping lengths for tetrahedral site ( $d_A$ ) and for octahedral site ( $d_B$ ) were calculated using the following relation [13]:

$$d_A = 0.25a\sqrt{3}, \quad d_B = 0.25a\sqrt{2} \quad (3)$$

In the case of lithium ferrites under investigation in this study, lithium ions occupy B-sites only whereas Co and Fe ions occupy both A and B sites.

To carryout the thermoelectric power studies, the sample was made into a pellet. A silver paint was applied on both the surfaces of the pellet to ensure good electric contact, and the pellet was held between two electrodes of a specially designed sample holder. A temperature difference (10 K) between two end surfaces of a semiconducting ferrite sample develops a thermo electromotive force (emf) across the sample. The thermoelectric power or Seebeck coefficient ( $S$  or  $\alpha$ ) is calculated using the following relation [14]:

$$S = \frac{\Delta E}{\Delta T} \quad (\mu\text{V/K}) \quad (4)$$

where  $\Delta E$  is the thermo emf produced across the two ends of the sample, and the temperature difference between the two surfaces ( $\Delta T$ ) of the pellet was maintained at 10 K.

The carrier concentration values of the prepared samples were calculated using the following relation [15]:

$$n = Ne^{-se/K} \quad (5)$$

where  $S$  Seebeck coefficient,  $e$  charge of electron,  $K$  Boltzmann constant, and  $N$  concentration of electronic levels involved in the conduction process. Ferrites are low-mobility semiconductors having exceedingly narrow local sized levels, so the value of  $N$  can be taken as  $10^{22}/\text{cc}$  [15].

Structural/microstructural, thermoelectric power studies of the citrate-gel prepared nanocrystalline Li–Co ferrites have been carried out, and the results are discussed.

## XRD studies

The XRD patterns of the prepared samples are shown in Fig. 1, which reveal the formation of a single-phase cubic spinel structure without any extra impurity peak as confirmed by comparing the same with the reference data from JCPDS card number 00-013-0207. From these patterns, it is concluded that there was no change in the basic crystal structure of Li ferrites on substitution of  $\text{Co}^{2+}$  ions.



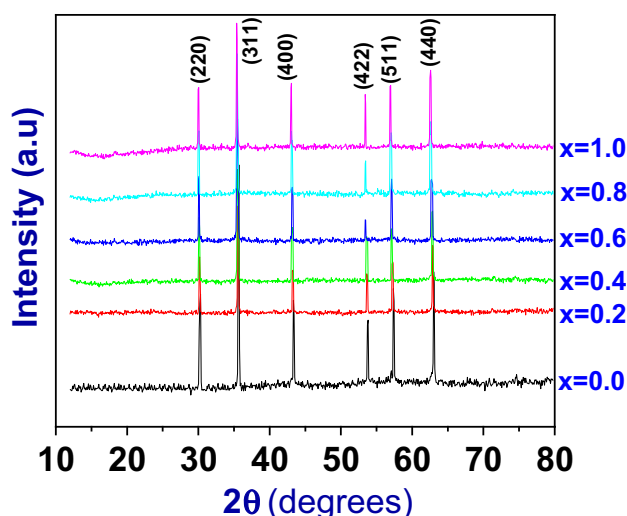


**Fig. 1** XRD pattern of the  $[\text{Li}_{0.5}\text{Fe}_{0.5}]_{1-x}\text{Co}_x\text{Fe}_2\text{O}_4$  nanoferrites with  $x = 0.0, 0.2, 0.4, 0.6, 0.8$ , and  $1.0$

**Table 1** Structural parameters of  $[\text{Li}_{0.5}\text{Fe}_{0.5}]_{1-x}\text{Co}_x\text{Fe}_2\text{O}_4$  nanoferrites

Ferrite composition	Crystallite size (nm)	Lattice parameter $a$ (Å)	$d_A$	$d_B$
$\text{Li}_{0.5}\text{Fe}_{2.5}\text{O}_4$	41.90	8.356	3.618	2.95
$\text{Li}_{0.4}\text{Co}_{0.2}\text{Fe}_{2.4}\text{O}_4$	43.01	8.370	3.624	2.959
$\text{Li}_{0.3}\text{Co}_{0.4}\text{Fe}_{2.3}\text{O}_4$	38.44	8.375	3.626	2.960
$\text{Li}_{0.2}\text{Co}_{0.6}\text{Fe}_{2.2}\text{O}_4$	37.57	8.386	3.631	2.964
$\text{Li}_{0.1}\text{Co}_{0.8}\text{Fe}_{2.1}\text{O}_4$	37.06	8.395	3.635	2.967
$\text{CoFe}_2\text{O}_4$	36.90	8.404	3.639	2.971

The average crystallite sizes of the prepared Li–Co ferrites of different compositions have been estimated from the XRD line width of the most intense peak (311) using Debye–Scherrer’s formula and were found to be in the range of 36–43 nm as evidenced from Table 1. Lattice parameter and hopping length of the prepared ferrites were calculated from the Eqs. 2 and 3, and the values are tabulated in Table 1. It is observed that there is an increase in the lattice parameter ( $a$ ) with the increase in cobalt content in Li ferrites as shown in Fig. 2, which obeys Vegard’s law [16].

The increase in the lattice parameter with the increasing Co concentration was attributed to the larger ionic radius of  $\text{Co}^{2+}$  ion (0.82 Å) compared to those of  $\text{Li}^{1+}$  ion (0.74 Å) and  $\text{Fe}^{3+}$  ion (0.64 Å) [16] in which substitution by the larger ions results in the expansion of the lattice. All the three ions are associated with the coordination number 6. Hopping length has also increased with Co composition as evidenced by Table 1, because it is directly proportional to lattice parameter.

## TEM studies

The morphology and particle size of the citrate-gel prepared nanocrystalline Li–Co ferrite sample powders were observed by transmission electron microscopy (TEM). The bright-field TEM images of  $[\text{Li}_{0.5}\text{Fe}_{0.5}]_{1-x}\text{Co}_x\text{Fe}_2\text{O}_4$  powders where  $x = 0.0, 0.2, 0.4, 0.6, 0.8$ , and  $1.0$  calcined at  $500^\circ\text{C}$  are shown in Fig. 3 in which the average particle size observed was  $\sim 30$  nm. Hence, TEM analysis and XRD analysis confirm the nanoscale nature of the prepared samples. TEM images show the homogeneous distribution of the particles, and a few of them are in agglomerated form. The fact that the agglomeration of particles lies in nanometric region was evidenced by TEM images.

## FTIR Studies

The room-temperature FTIR spectra of Li–Co series  $[\text{Li}_{0.5}\text{Fe}_{0.5}]_{1-x}\text{Co}_x\text{Fe}_2\text{O}_4$  (where  $x = 0.0, 0.2, 0.4, 0.6, 0.8$ , and  $1.0$ ) are shown in Fig. 4. The FTIR spectra were found to exhibit two major bands  $\nu_1$  and  $\nu_2$  in range of  $400\text{--}600\text{ cm}^{-1}$ . The well-defined sharp absorption bands in the FTIR spectrum establish the formation of ferrites in the sample [17].

The first absorption band  $\nu_1$  around  $490\text{--}500\text{ cm}^{-1}$  has appeared due to the vibrations of  $\text{Fe}^{3+}\text{--O}$  bond in the tetrahedral sites (A-sites). The second absorption band  $\nu_2$  observed around  $400\text{--}425\text{ cm}^{-1}$  was due to the vibration of  $\text{Fe}^{3+}\text{--O}$  bond in the octahedral sites (B-sites). The third band  $\nu_3$  observed at nearly  $450\text{ cm}^{-1}$  can be attributed to the Li–O vibrations [18]. In Li–Co ferrites, cobalt ions are distributed randomly between the tetrahedral and octahedral sites; hence,  $\nu_1$  and  $\nu_2$  themselves indicate the Co–O

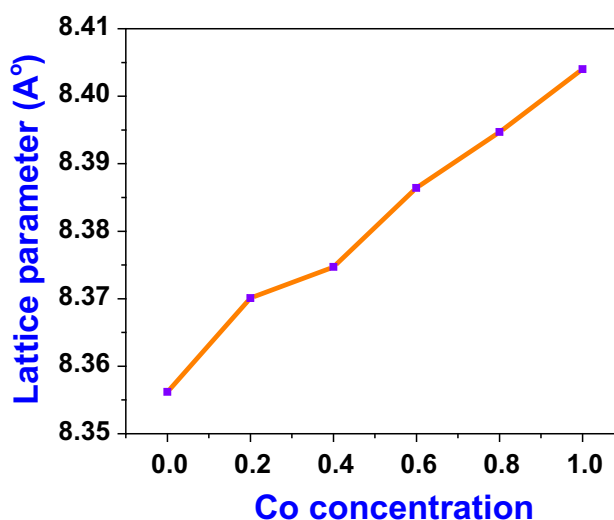


**Fig. 2** Variation of Lattice parameter of Li–Co nanoferrites with Co concentration



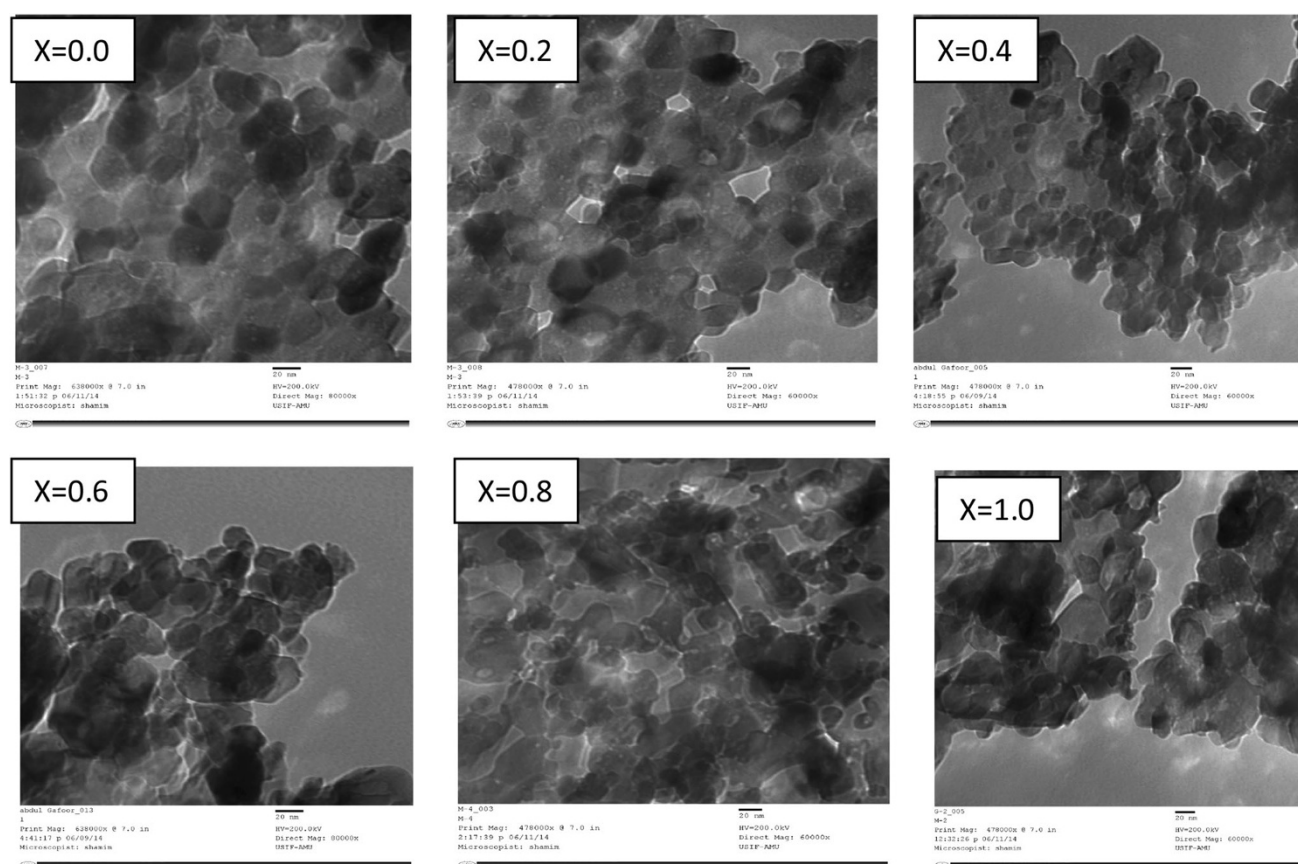


**Fig. 3** TEM image of  $[\text{Li}_{0.5}\text{Fe}_{0.5}]_{1-x}\text{Co}_x\text{Fe}_2\text{O}_4$  powders where  $x = 0.0, 0.2, 0.4, 0.6, 0.8$ , and  $1.0$

band. Similar results were reported earlier [15]. The band  $\nu_3$  can also show the presence of the lithium in the prepared sample, and upon increasing the Co concentration, the third band  $\nu_3$  disappears due to less amount of lithium as evidenced in the samples with  $X = 0.8$  and  $X = 1.0$ . The values of  $\nu_1$ ,  $\nu_2$ , and  $\nu_3$  are summarized in Table 2.

#### Thermoelectric power studies

The thermoelectric power studies of the prepared nanocrystalline Li–Co ferrites were measured by the differential method in the temperature range of 200–600 °C. The thermo e.m.f of the samples was measured during cooling cycle, because during cooling the sample attains more thermal stability than during heating. The values of the Seebeck coefficient of the mixed Li–Co nanoferrites under study were calculated from the observed values of the thermo e.m.f and are summarized in Table 3. Carrier concentration of the prepared samples was calculated at Curie temperature. From the Table 3 one can observe that Seebeck coefficient increases with the increasing Co concentration. This may be attributed to the fact that by increasing the Co concentration, cobalt ions occupy the

B-sites and transfer the  $\text{Fe}^{3+}$  ions to the A-site resulting in a decrease in  $\text{Fe}^{3+}$  ions in the B-site. This fact leads to the decrease in  $\text{Fe}^{2+}$  ions in the B-site. However, according to Srinivasan [19], Seebeck coefficient  $S$  for cubic system is given by

$$S = \frac{\text{Total number of iron ions on B - sites/}}{\text{total number of Fe}^{2+} \text{ ions B - sites}}$$

with the increasing Co content as the number of  $\text{Fe}^{2+}$  ions on B-sites decreases,  $S$  increases in the lithium ferrites which can be justified from the above expression of  $S$ .

Due to the above mentioned reason, with the increasing Co content, a large numbers of charge carriers are produced so that more energy is needed to transfer the charge carriers between the different cations. Hence, large emf is produced, which enhances the thermoelectric power.

Figure 5 shows the variation of Seebeck coefficient with temperature for all the prepared samples. It can be seen from the Fig. 5 that the sign of Seebeck coefficient was positive at low temperature. By increasing the temperature, Seebeck coefficient attained negative value for all the ferrites under investigation. This indicates that, at low temperature, these prepared samples behave like p-type semiconductors.



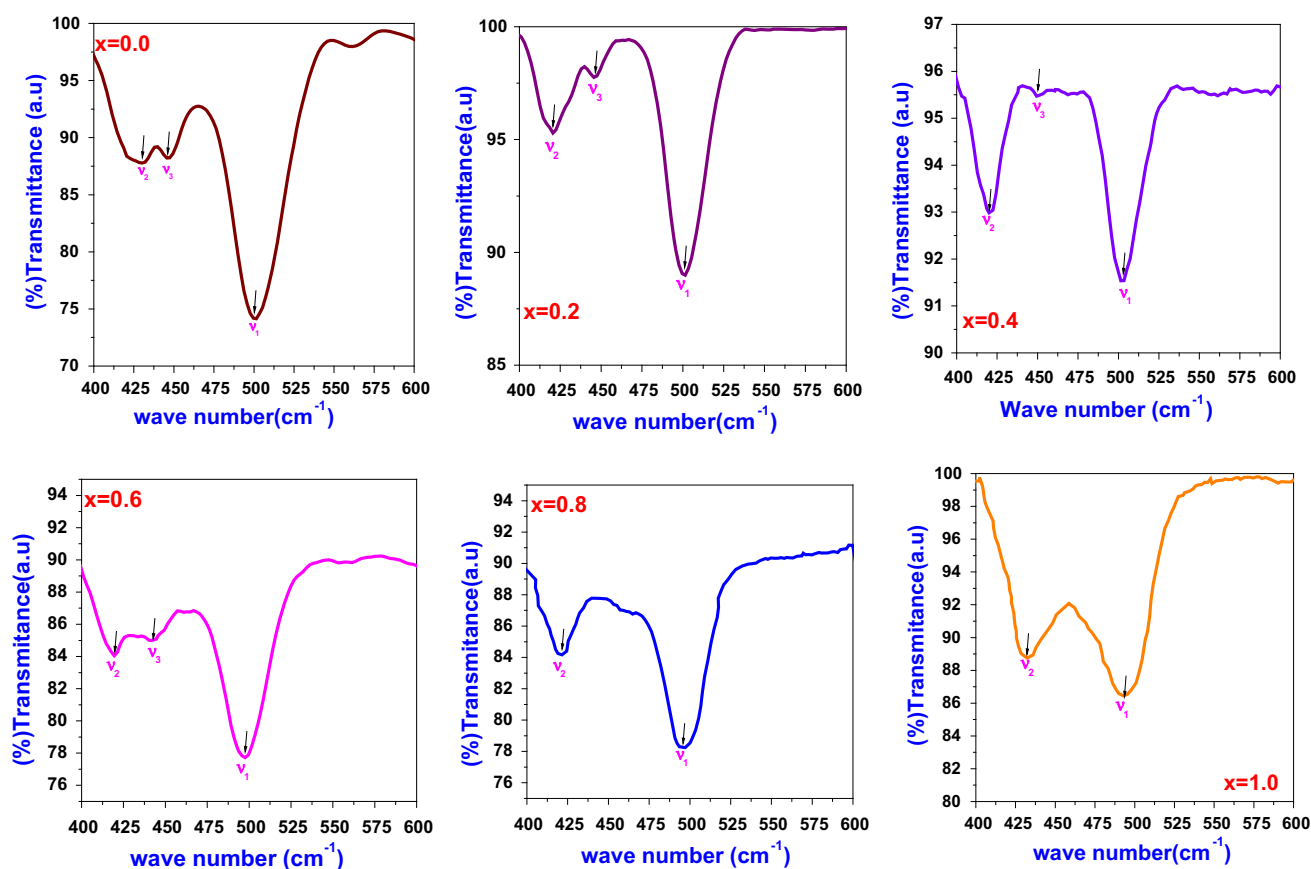


**Fig. 4** FTIR spectra of  $[\text{Li}_{0.5}\text{Fe}_{0.5}]_{1-x}\text{Co}_x\text{Fe}_2\text{O}_4$  nanoferrites with  $x = 0.0, 0.2, 0.4, 0.6, 0.8$ , and  $1.0$

**Table 2** FTIR parameters of Li–Co ferrites

S. No	Ferrite composition	$\nu_1$ ( $\text{cm}^{-1}$ )	$\nu_2$ ( $\text{cm}^{-1}$ )	$\nu_3$ ( $\text{cm}^{-1}$ )
1	$\text{Li}_{0.5}\text{Fe}_{2.5}\text{O}_4$	501	430	446
2	$\text{Li}_{0.4}\text{Co}_{0.2}\text{Fe}_{2.4}\text{O}_4$	500	421	445
3	$\text{Li}_{0.3}\text{Co}_{0.4}\text{Fe}_{2.3}\text{O}_4$	499	419	443
4	$\text{Li}_{0.2}\text{Co}_{0.6}\text{Fe}_{2.2}\text{O}_4$	497	418	441
5	$\text{Li}_{0.1}\text{Co}_{0.8}\text{Fe}_{2.1}\text{O}_4$	494	420	—
6	$\text{CoFe}_2\text{O}_4$	492	431	—

**Table 3** Seebeck Coefficient, Curie temperature and Carrier concentration of the prepared  $[\text{Li}_{0.5}\text{Fe}_{0.5}]_{1-x}\text{Co}_x\text{Fe}_2\text{O}_4$  with  $x = 0.0, 0.2, 0.4, 0.6, 0.8$ , and  $1.0$

Composition	Curie temperature (K)	Seebeck coefficient (S) ( $\mu\text{V/K}$ ) at $T_c$	Carrier concentration at $T_c$
$\text{Li}_{0.5}\text{Fe}_{2.5}\text{O}_4$	>873	—	—
$\text{Li}_{0.4}\text{Co}_{0.2}\text{Fe}_{2.4}\text{O}_4$	861	−3546	$1.64 \times 10^{20}$
$\text{Li}_{0.3}\text{Co}_{0.4}\text{Fe}_{2.3}\text{O}_4$	840	−4413	$0.65 \times 10^{20}$
$\text{Li}_{0.2}\text{Co}_{0.6}\text{Fe}_{2.2}\text{O}_4$	815	−4958	$0.32 \times 10^{20}$
$\text{Li}_{0.1}\text{Co}_{0.8}\text{Fe}_{2.1}\text{O}_4$	801	−5840	$0.11 \times 10^{20}$
$\text{CoFe}_2\text{O}_4$	790	−6140	$0.08 \times 10^{20}$

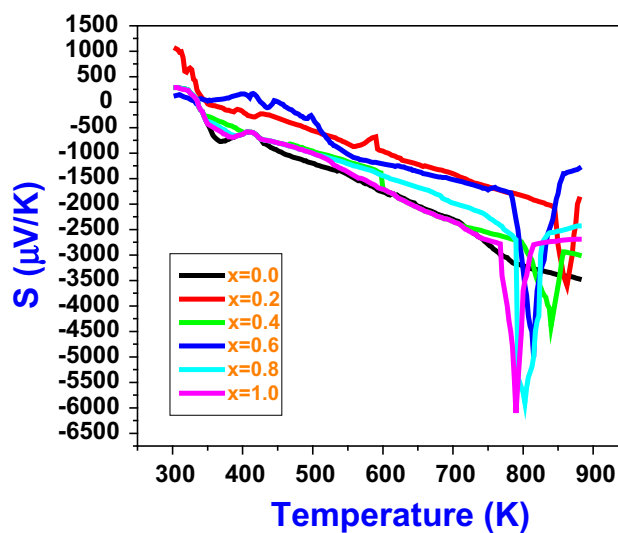


**Fig. 5** Variation of Seebeck coefficient ( $S$ ) with temperature for Li–Co ferrites

By increasing the temperature, the predominant conduction mechanism in these ferrites was due to the electrons and the behave like n-type semiconductors. Such type of conductivity is attributed to the hopping of electrons between  $\text{Fe}^{2+}$





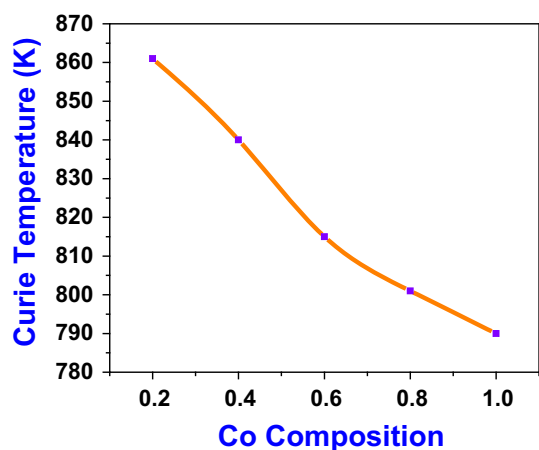
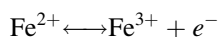


**Fig. 6** Variation of Curie temperature with Co composition in Li–Co ferrites

and  $\text{Fe}^{3+}$  ions at octahedral sites. The n-type of conducting mechanism can be shown as below:



It can be seen that the values of the Seebeck coefficient for all mixed nanocrystalline Li–Co ferrites increases with the increasing temperature which indicates that more n-type charge carriers (electrons) were released with the increasing temperature. Further increase in the temperature results in a decrease in Seebeck coefficient which remains almost constant later on. This temperature at which there is a sudden change in  $S$  value was named  $T_c$ . From the Fig. 5, the  $T_c$  of all the ferrite samples were measured and are tabulated in Table 3. Ferrites after reaching the  $T_c$  become paramagnetic; hence, there is no probability for the hopping of electrons between A-site and B-site beyond  $T_c$ . Thus,  $S$  becomes constant after  $T_c$  [20]. The  $T_c$  of pure lithium ferrite was around 630 °C (903 K) [21]. In the present case, the thermoelectric power measurements were carried out in the temperature range of 200–600 °C (473–873 K) using the differential method. Hence, the  $T_c$  is not observed in the Fig. 5, i.e., the  $T_c$  of the pure lithium ferrite was beyond the measured temperature range and is mentioned in the Table 3 as >873 K.

It is clear that in case of Li–Co nanoferrites, the non-magnetic property (thermoelectric power) under study was exhibiting a well-defined transition at the Curie temperature, like the magnetic properties, viz., susceptibility, permeability, and spontaneous magnetization. The fact that the value of Seebeck coefficient shows minimum values at  $T_c$  indicates that the magnetic ordering has a marked influence on the thermoelectric power of these ferrite samples under investigation. From the present study, considering the semiconducting behavior of investigated ferrites, the charge carriers are considered to be localized at ions or at vacant sites as a result of electron–phonon interaction [22].

The variation of  $T_c$  with Co composition of the prepared samples was shown in Fig. 6. From the figure, it is clear that the  $T_c$  of the samples decrease with the increasing cobalt content. This may be due to the fact that as Co concentration increases, the  $\text{Fe}^{3+}$  ions decreases, which reduces the overall number of Fe ions in the B-Sites which in turn results in a decrease of A–B interaction  $\text{Fe}_A^{3+}\text{--O--Fe}_B^{3+}$ . Hence, thermal energy required to offset the alignment of magnetic moment decreases leading to the decrease of  $T_c$  [22].

## Conclusions

The effect of cobalt substitution on structural and thermoelectric power properties of lithium ferrites was studied. By cobalt substitution, the lattice constant of the nanocrystalline Li–Co ferrites increases, which obeys the Vegard's law. The particle size from TEM image was nearly 20 nm, which confirms the formation of nanosized materials. In FTIR spectra, two significant absorption bands were observed, which confirm the formation of spinel ferrites. At low temperature, Seebeck coefficient was positive which indicates the p-type semiconducting behavior of the ferrites, and at higher temperature they act like a n-type semiconductor.

## Methods

### Synthesis

The starting materials are Lithium nitrate [ $\text{Li}(\text{NO}_3)$ ], Cobalt nitrate [ $\text{Co}(\text{NO}_3)_6\text{H}_2\text{O}$ ], Ferric nitrate [ $\text{Fe}(\text{NO}_3)_3 \cdot 9\text{H}_2\text{O}$ ], Citric acid [ $\text{C}_6\text{H}_8\text{O}_7\text{H}_2\text{O}$ ], and Ammonia [ $\text{NH}_3$ ] (98 % purity; SD Fine-chem limited, Mumbai, India). The chemicals were weighted in a stoichiometric proportion without any further purification. Nanocrystalline Li–Co ferrites were prepared by citrate-gel autocombustion method [13]. First of all, the stoichiometric quantities of metal nitrates were dissolved in a minimum quantity of distilled water, and an aqueous solution of citric acid was added to the metal nitrate solution. The pH of the solution was maintained at seven by addition of ammonia solution drop by drop and heated to 80 °C until a fluffy mixture was formed, and finally the fluffy mixture was dried, which results in a burn ash and which was calcinated at 500 °C for 4 h to ensure good densification and elimination of impurities. In this preparation method, the energy from the exothermic reaction between oxidant and reductant can be used to prepare the material in the nanoform with desirable phase in a short period of time.



## Characterization

The crystallographic structure/micro structure was investigated by using XRD analysis, FTIR, and TEM.

X-ray studies on the obtained powders were carried out by X-ray powder diffractometer (Rigaku Geiger Flex 3 kW diffractometer) using Cu K $\alpha$  radiation ( $\lambda = 1.5406 \text{ \AA}$ ) in a wide range of Bragg's angles  $2\theta$  ( $10^\circ < 2\theta < 80^\circ$ ) with scanning rate of  $2^\circ/\text{min}$ .

FTIR spectra of the prepared ferrites were recorded on a Perkin Elmer RX-1 FTIR spectrometer using KBr pellets in the range of  $600\text{--}400 \text{ cm}^{-1}$ .

The size and shape of the synthesized lithium–cobalt ferrite particles were analyzed by TEM (TEM, Philips CM12, Holland).

Thermoelectric power of the prepared samples was measured using the differential method.

**Acknowledgments** The authors are very grateful to Prof. K.Venu Gopal Reddy, Head, the Department of Physics, the University College of Science, Osmania University, Hyderabad. The authors are very thankful to the UGC, New Delhi, for their financial assistance through major research project (MRP).

**Conflict of interest** The authors declare that they have no competing interests.

**Author contributions** All the authors were involved with the whole research work presented here. The authors GA and AG have synthesized the nanoparticles and performed various tests. MRS and DR have helped in interpreting the data and communicating the article to the journal. VN has provided required facilities for measurements and discussed the obtained data. All the authors read and approved the final manuscript.

**Open Access** This article is distributed under the terms of the Creative Commons Attribution License which permits any use, distribution, and reproduction in any medium, provided the original author(s) and the source are credited.

## References

- Farhadi, S., Pourzare, K., Sadeghinejad, S.: Simple preparation of ferromagnetic  $\text{Co}_3\text{O}_4$  nanoparticles by thermal dissociation of the  $[\text{CoII}(\text{NH}_3)_6](\text{NO}_3)_2$  complex at low temperature. *J. Nanostruct. Chem.* **3**, 16 (2013)
- Baba, P.D., Argentina, G.M., Courtney, W.E., Dionne, G.F., Temme, D.H.: Fabrication and properties of Microwave Lithium ferrites. *IEEE Trans. Magn.* **8**, 83–94 (1972)
- Gabal, M.A., Ata-Allah, S.S.: Effect of the diamagnetic substitution on the structural, electrical and magnetic properties of the cobalt ferrites. *Mater. Chem. Phys.* **85**, 104–112 (2004)
- Kawazoe, H., Ueda, K.: Transparent conductive oxides based on the spinel structure. *J. Am. Ceram. Soc.* **82**, 3330–3336 (1999)
- Venugopal Reddy, P., Sheshagiri rao, T.: X-ray studies on lithium–nickel and manganese–magnesium mixed ferrites. *J. Less-Comm. Mater.* **75**, 255–1980 (1980)
- Roy, P.K., Bera, J.: Effect of Mg substitution on electromagnetic properties of  $\text{Ni}_{0.25}\text{Cu}_{0.2}\text{Zn}_{0.55}\text{Fe}_2\text{O}_4$  ferrite prepared by auto combustion method. *J. Magn. Magn. Mater.* **298**, 38–42 (2006)
- Raghasudha, M., Ravinder, D., Veerasomaiah, P.: Magnetic properties of Cr-substituted Co-ferrite nanoparticles synthesized by citrate-gel auto combustion method. *J. Nanostruct. Chem.* **3**, 63 (2013)
- Leis, M.F.F., Porto, A.O., Goncalves, C.M., Fabris, J.D.: Cation occupancy sites in synthetic Co-doped magnetites as determined with X-ray absorption (XAS) and Mossbauer spectroscopies. *J. Magn. Magn. Mater.* **278**, 263–269 (2004)
- Al-Hilli, M.F., Li, S., Kassim, K.S.: Microstructure, electrical properties and Hall coefficient of europium doped Li–Ni ferrites. *Mater. Sci. Engg. B* **158**, 1–6 (2009)
- Liu, C., Lan, Z., Jiang, X., Yu, Z., Sun, K., Li, L., Liu, P.: Effects of sintering temperature and  $\text{Bi}_2\text{O}_3$  content on microstructure and magnetic properties of Li–Zn ferrites. *J. Magn. Magn. Mater.* **320**, 1335–1339 (2008)
- Rodrigues, H.O., PiresJunior, G.F.M., Almeida, J.S., Sancho, E.O., Ferreira, A.C., Silva, M.A.S., Sombra, A.S.B.: Study of the structural, dielectric and magnetic properties of  $\text{Bi}_2\text{O}_3$  and PbO addition on  $\text{BiFeO}_3$  ceramic matri. *J. Phys. Chem. Solids* **71**, 1329–1336 (2010)
- Ravi kumar, B., Ravinder, D.: TEP studies of Gd substituted Mn–Zn ferrites. *Mater. Lett.* **53**, 441–445 (2002)
- Raghasudha, M., Ravinder, D., Veerasomaiah, P.: Characterization of nano-structured magnesium–chromium ferrites by Citrate-gel auto combustion method. *Adv. Mat. Lett.* **4**, 910–916 (2013)
- Raghasudha, M., Ravinder, D., Veerasomaiah, P.: Thermoelectric power studies of Co–Cr nano ferrites. *J. Alloys Comp.* **604**, 276–280 (2014)
- Morin, F.J., Geballe, T.H.: Electrical conductivity and Seebeck effect in  $\text{Ni}_{0.80}\text{Fe}_{2.20}\text{O}_4$ . *Phys. Rev.* **99**, 467–498 (1955)
- Cahn, R.W.: *Physical Metallurgy*. North Holland Physics Publishing, North-Holland, Amsterdam (1985)
- Wang, F.F.Y.: Physical and Chemical properties of Garnets. *Treatise Mater. Sci. Technol.* **2**, 279–384 (1973)
- Sankaranarayan, V.K., Prakash, O., Pant, R.P., Islam, M.: Lithium ferrite nano particles for ferro fluid applications. *J. Magn. Magn. Mater.* **252**, 7–9 (2002)
- Srinivasan, G., Srivastava, C.M.: Electrical conductivity mechanism in zinc and copper substituted magnetite. *Phys. Status Solidi B* **108**, 665–671 (1981)
- Ravinder, D., Ramana Reddy, A.V.: Electrical & transport properties of zinc substituted manganese ferrites. *Mater. Lett.* **38**, 265–269 (1999)
- Al-Hilli, M.F., Li, S., Kassim, K.S.: Gadolinium substitution and sintering temperature dependent electronic properties of Li–Ni ferrites. *Mater. Chem. Phys.* **128**, 127–132 (2011)
- Haberey, F., Wijn, H.P.J.: Effect of temperature on the dielectric relaxation in polycrystalline ferrites. *Phys. Status Solidi B* **26**, 231–240 (1968)

